Disruption of AtHAK/KT/KUP9 enhances plant cesium accumulation under low potassium supply.

Laure Genies, Ludovic Martin, Satomi Kanno, Serge Chiarenza, Loic Carasco, Virginie Camilleri, Alain Vavasseur, Pascale Henner, Nathalie Leonhardt

Disruption of *AtHAK/KT/KUP9* enhances plant cesium accumulation under low potassium supply.

Laure Genies[1,2,*], Ludovic Martin[1], Satomi Kanno[1], Serge Chiarenza[1], Loïc Carasco[2], Virginie Camilleri[3], Alain Vavasseur[1], Pascale Henner[2,*], Nathalie Leonhardt[1,*]

[1]Aix Marseille University, French Alternative Energies and Atomic Energy Commission (CEA), National Center for Scientific Research (CNRS), Bioscience and Biotechnology Institute of Aix-Marseille (BIAM), Laboratory of Signaling for the Adaptation to their Environment (SAVE), France F-13108

[2]Laboratory of research on radionuclides transfer within terrestrial ecosystems (LR2T), Institute for Radiological protection and Nuclear Safety (IRSN), 13115 Cadarache, France

[3]Laboratory for Radionuclide Ecotoxicology (LECO), Institute for Radiological protection and Nuclear Safety (IRSN), 13115 Cadarache, France

*Corresponding authors: laure.genies@gmail.com; pascale.henner@irsn.fr; nathalie.leonhardt@cea.fr

Abstract

Understanding the molecular mechanisms that underlie cesium (Cs^+) transport in plants is important to limit the entry of its radioisotopes from contaminated areas into the food chain. The potentially toxic element Cs^+, which is not involved in any biological process, is chemically closed to the macronutrient potassium (K^+). Among the multiple K^+ carriers, the high-affinity K^+ transporters family HAK/KT/KUP is thought to be relevant in mediating opportunistic Cs^+ transport. Of the 13 *KUP* identified in *Arabidopsis thaliana*, only *HAK5*, the major contributor to root K^+ acquisition under low K^+ supply, has been functionally demonstrated to be involved in Cs^+ uptake *in planta*. In the present study, we showed that accumulation of Cs^+ increased by up to 30% in two *A. thaliana* mutant lines lacking *KUP9* and grown under low K^+ supply. Since further experiments revealed that Cs^+ release from contaminated plants to the external medium is proportionally lower in the two *kup9* mutant alleles, we proposed that *KUP9* disruption could impair Cs^+ efflux. By contrast, K^+ status in *kup9* mutants is not affected, suggesting that *KUP9* disruption does not alter substantially K^+ transport in experimental conditions used. The putative primary role of KUP9 in plants is further discussed.

Introduction

Cesium is an alkali metal generally occurring at low concentrations in soil solution, predominantly as the monovalent cation Cs^+ (Greenwood and Earnshaw 1997). Although it has not been implicated in any biological process to date, Cs^+ is taken up by plants and can even be toxic (Hampton et al. 2004). Due to its low environmental concentration, the chemical toxicity of stable Cs^+ is rarely relevant in natural conditions (White and Broadley 2000). By contrast, the radiological threat of ^{134}Cs and ^{137}Cs, two radioisotopes of Cs^+ originated from nuclear activities, is a concern for the environment and human health in contaminated areas. These two β- and γ-emitting radionuclides are among those unintentionally released at harmful levels during nuclear accidents, including those at Fukushima (Japan, 2011) and Chernobyl (Ukraine, 1986) (Steinhauser et al. 2014) and remain monitored due to their relative long half-lives (2.06 and 30.17 years for ^{134}Cs and ^{137}Cs, respectively). Contaminated food is regarded as a major source of radionuclides exposure for humans after the initial phase of a nuclear accident (Hamada and Ogino 2012). Therefore, understanding the transfer of radiocesium in plants remains a challenging question for reducing its transfer into the food chain through the development of "safe crops" which accumulate lower amounts of radionuclides or through phytoremediation strategies to remove Cs^+ from soils (White and Broadley 2000).

To date, it is commonly admitted that plants do not discriminate significantly between stable and radioactive isotopes of Cs^+ (White and Broadley 2000), which are used indifferently for uptake experiments. Cs^+ shares closed chemical properties with the macronutrient K^+ (Bowen 1979), and early studies demonstrated that mechanisms underlying Cs^+ and K^+ uptake in plants are similar (Collander 1941, Epstein and Hagen 1952). As for K^+, Cs^+ uptake in plants can be divided into two major systems: a high-affinity transport system (HATS) operating for external Cs^+ concentration in the micromolar range and a low-affinity transport system (LATS) operating in the millimolar range (Bange and Overstreet 1960, Shaw and Bell 1989). In addition, several studies on different plant species described a competitive effect of external K^+ on Cs^+ uptake (Kondo et al. 2015, Middleton et al. 1960, Sacchi et al. 1997, Smolders et al. 1996). Since Cs^+ has no relevant physiological role in plants and given the above-mentioned evidence suggesting that K^+ and Cs^+ share the same transport mechanisms, it is generally assumed that Cs^+ entry in plants is mainly mediated through K^+ transporters (White and Broadley 2000).

Multiple transport systems are involved in plant K^+ acquisition, and the contribution of each individual system depends on the external K^+ concentration (Alemán et al., 2011). In the same way, K^+ supply also affects the contribution of each pathway mediating Cs^+ uptake. In the model plant *Arabidopsis thaliana*, Non-selective Cation Channels (NSCCs) are assumed to mediate a significant part of Cs^+ uptake under sufficient K^+-supply (Hampton et al. 2005, White and Broadley 2000). The *Arabidopsis* Zinc-Induced-Facilitator-Like-2 (ZIFL2) carrier is also involved in Cs^+ partitioning in K^+-replete

plants (Remy et al., 2015). In contrast, the Shaker channel AKT1, which is a major contributor of K^+ uptake in roots of *A. thaliana* (Hirsch et al. 1998), is Cs^+-sensitive (Bertl et al. 1997) but is not relevant for plant Cs^+ uptake (Broadley et al. 2001).

In K^+-starved plants, transporters encoded by the *HAK/KT/KUP* (High-Affinity K^+-transporters/K^+-transporters/K^+-Uptake Permeases) genes family (named *KUP* in the following) have been pointed out as a relevant pathway for Cs^+ (Rubio et al. 2000, White and Broadley 2000). This statement is supported by numerous evidences, among those the role of bacterial KUP transporters in Cs^+ uptake (Bossemeyer et al. 1989), the demonstration that Cs^+ uptake in maize roots is mediated by K^+ HATS (Sacchi et al. 1997), which involve members of the *KUP* family (Alemán et al. 2011), the transport of Cs^+ through plants KUP transporter expressed in yeast (*AtHAK5*, Rubio et al. 2000) and in bacteria (*AtKUP9*, Kobayashi et al. 2010).

In *A. thaliana*, 13 genes encode for the KUP transporters (Mäser et al. 2001) among those only the high-affinity K^+ transporter HAK5 (Gierth et al. 2005, Rubio et al. 2000) has been demonstrated to be functionally involved in Cs^+ uptake (Qi et al. 2008). In the present study, we investigated the role of the KUP9 transporter in Cs^+ accumulation in *A. thaliana*. This transporter has been demonstrated to be involved in Cs^+ influx when expressed in an *Escherichia coli* mutant defective in K^+ transport systems (Kobayashi et al. 2010), and a recent work mentions a higher accumulation of Cs^+ in one *kup9* mutant (Adams et al. 2019). Using *A. thaliana* mutants disrupted in the *KUP9* gene, we provide *in planta* evidence that KUP9 play a significant role in Cs^+ accumulation, whereas its disruption does not substantially alter plant K^+ content.

Materials and Methods

Plant materials

Arabidopsis thaliana ecotype Columbia-0 (Col-0) was used as the wild-type. Consequences of a disruption of *KUP9* (At4g19960) was studied using two independent *kup9* T-DNA insertion lines obtained from the SAIL (N862313) and the SALK (N670022) collections, respectively. T-DNA insertion was checked, and homozygous lines were identified using a combination of T-DNA border primers and gene specific primers as outlined in the online protocol “Screening SALK T-DNA mutagenesis lines” (University of Wisconsin, Madison Knockout Facility and Ohio State University, Arabidopsis Biological Resource Center (https://www.mcdb.ucla.edu/Research/Goldberg/HC70AL_S06/pdf/Expt6protocol.pdf). The SALK_108080C mutant line, in which the T-DNA insertion is located in exon 9, has previously been introduced by Adams et al. (2019) to evaluate the contribution of KUPs to K^+ and Cs^+ accumulations in Arabidopsis. According to Tenorio-Berrío et al. (2018), the SALK_108080C mutant line is named

kup9-1. The *kup9-3* allele corresponds to the SAIL_211_E04 mutant line, in which T-DNA insertion is located in intron 2 (the *kup9-2* allele already refers to another mutant line previously characterized in Tenorio-Berrío et al. 2018).

Growth conditions

Arabidopsis seeds were surface-sterilized using a mix of 70% ethanol (v/v) / 0.05% SDS (v/v) and rinsed in ethanol 96% before sowing in Petri dishes (120 × 120 mm) on a half-strength Murashige and Skoog medium (MS½, Murashige and Skoog 1962) containing 1% (w/v) agar and 1% (w/v) sucrose. The sowing boxes were placed at 4°C for 48 h before transfer in a growth chamber set to 23°C, 50% relative humidity with 8 /16 h day/night cycle. Then, 7 days-old seedlings were transferred on sand (Zolux) watered with a solution (pH 5.8) containing 1.1 mM $MgSO_4$, 805 µM $Ca(NO_3)_2$, 2 mM KNO_3, 60 µM K_2HPO_4, 695 µM KH_2PO_4 and micronutrients (3.6 µM $MnSO_4$, 74 nM $(NH_4)_6Mo_7O_{24}$, 3 µM $ZnSO_4$, 9.25 µM H_3BO_3, 785 nM $CuSO_4$, 20 µM Na_2EDTA and 20 µM $FeSO_4$). Finally, 21 days-old plants were transferred on 1 L of this solution during 3-5 days for acclimation to hydroponics growing.

In subsequent experiments, basic composition of the nutritive media with controlled K^+ and Cs^+ content is: 0,75 mM $MgSO_4$, 2 mM $Ca(NO_3)_2$, 0,5 mM H_3PO_4, 3,5 mM MES, 10 µM Fe-EDTA, 3,6 µM $MnSO_4$, 74 nM $(NH_4)_6Mo_7O_{24}$, 3 µM $ZnSO_4$, 9,25 µM H_3BO_3, 785 nM $CuSO_4$, pH adjusted to 5.8 with NMDG (and 1% (w/v) agar for agar plates only). K^+ and Cs^+ concentrations on the different conditions were adjusted with KCl and CsCl.

We defined three distinct levels of K^+ supplied to plants: low (10 µM K^+); intermediate (100 µM K^+); sufficient (1000 µM or 3000 µM K^+ in experiments described in this paper). These concentrations have been chosen according to different models established to describe the different contributions and functioning of K^+ transporters depending on external K^+ concentration in the literature (Alemán et al. 2014, Nieves-Cordones et al. 2019).

K^+, Rb^+ and Cs^+ accumulation in seedlings

Accumulation experiments in plants were performed under hydroponics conditions using the nutritive solution described above. Protocol for long-term Cs^+ accumulation assays in hydroponics conditions is described elsewhere (Genies et al. 2017). Briefly, after acclimation to hydroponics, 25 days-old (± 1 day) plants were grown in 10 or 3000 µM K^+- solution for 5 days and then exposed for 7 days to 1 µM Cs^+. To alleviate the detrimental effects of changing the solution composition, K^+ concentration remained the same before and during exposure to Cs^+. Some plants remained in the Cs^+-free solution to analyze K^+-content after growing in 10, 100 or 3000 µM K^+-solution. The solutions were renewed every 2-3 days to avoid significant depletion in the medium due to uptake by plants.

For the Rb^+ uptake experiments, 30 days-old plants supplied with 10 µM K^+-solution for 7 days were transferred in 20 mL of a K^+-free solution containing 50 µM RbCl. After 7 h, roots were rinsed with Rb^+-free solution to remove adsorbed Rb^+.

Cs^+ toxicity assay

For evaluation of the Cs^+ effects on cotyledons development, surface-sterilized Arabidopsis seeds of Col-0, *hak5-3* (Qi et al. 2008), *kup9-1* and *kup9-3* were sown on 2 mL of nutritive solution containing 10 µM or 1000 µM K^+. After 48h at 4°C, 1 mL of nutritive solution contaminated with CsCl (final concentration ranging from 0 to 300 µM) was added and plants were allowed to grow for 7 days in a growth chamber.

For evaluation of the Cs^+ effects on roots elongation**,** surface-sterilized *Arabidopsis* seeds of Col-0, *hak5-3*, *kup9-1* and *kup9-3* were sown and allowed to grow in MS½ agar plates vertically oriented during 4 days in order to avoid effects of K^+ treatments on germination. Seedlings were then transferred under sterile conditions on different agar media containing low or sufficient K^+ and Cs^+ (0, 10, 100, 300 or 500 µM). Analysis of agar media revealed that K^+ concentrations were between 14 and 40 µM and around 1000 µM in low and sufficient K^+ conditions, respectively. Primary root elongation was measured after 7 days on these plates, oriented vertically.

Cs^+ fluxes between seedlings and external solution

The protocol for the Cs^+ depletion experiments was adapted from the Rb^+ depletion experiments described in Rubio et al. (2008). Thirty days-old plants, supplied with 10 µM K^+-solution for 7 days to stimulate Cs^+ uptake, were transferred to 20 mL of a K^+-free solution containing 60 µM CsCl. At different time points, 100 µL of this Cs^+-contaminated solution were sampled to follow Cs^+ depletion due to plant Cs^+ uptake. Then, Cs^+ contaminated plants were transferred to 20 mL of a 10 µM K^+-nutrient solution containing no Cs^+ after prior rinsing in this solution to remove adsorbed Cs^+ bound to the roots. At different time points, 100 µL of this Cs^+-free solution were sampled to follow Cs^+ released from plants to the external medium.

At the beginning of the Cs^+ release experiment, the Cs^+ content in each individual plant was assessed as the missing amount of Cs^+ in the solution at the end of the Cs^+ depletion experiment. During the Cs^+ release experiment, the percentage of Cs^+ released for each plant was calculated by dividing the Cs^+ content measured in the depletion solution at each time-point by the assessed Cs^+ content in the plant at the beginning of the release experiment.

Measure of Cs^+, K^+ and Rb^+

Plants and aliquots of exposure solutions and agar media were analyzed, measuring and verifying the K^+, Cs^+ and Rb^+ concentrations. For plant samples, roots and shoots were separated, blotted on Benchkote paper and then oven dried (3-5 days at 50-60°C). Aliquots (5 mL) of agar media and dried plant matters were mineralized in HNO_3 65% (5 or 10 mL for plants and agar media, respectively) and H_2O_2 30% (1.5 or 3 mL) at 100-150°C in a sand bath. Mineralisates were evaporated to dryness and redissolved in HNO_3 2% v/v prior to analysis.

In all substrates, Rb^+ and Cs^+ were quantified by ICP-MS (Inductively Coupled Plasma-Mass Spectrometry, PQ Excell Thermo Electron with S-Option, detection limit 5 $ng.L^{-1}$) and K^+ content by ICP-AES (-Atomic Emission Spectrometry, OPTIMA 8300, Perkin Elmer, quantification limit 10 $\mu g.L^{-1}$).

Spatial transcription profiling of KUP9

The fragment of 2745 bp upstream of the start codon of the *KUP9* gene was PCR amplified (forward primer: CCAATGTAACGAGGGAAGAGACT, reverse primer: CAGGGGAATTTCGAGTTCTTTTGT) and then inserted into pCR-XL-TOPO® vector. This first step allowed us to enhance subsequent amplification with *att*B primers (*att*B1 forward primer: *GGGGACAAGTTTGTACAAAAAAGCAGGCTAT*TGTAACGAGGGAAGAGACTTG, *att*B2 reverse primer: *GGGGACCACTTTGTACAAGAAAGCTGGGTC*TTTTGTAACAAAAGAACTCGAAATTC) for *KUP9* promoter cloning using Gateway® technology. Following the manufacturer's instructions, *KUP9* promoter was introduced into the entry vector pDONR221™ and then cloned in pBGWFS7 plasmid containing a *GFP-GUS* fusion. The construct was introduced into *Agrobacterium tumefaciens* (C58C1) and transformed into Col-0 plants using the floral dip method (Clough and Bent 1998). Staining of GUS activity was performed on T3 homozygous transgenic plants incubating tissues on a fixation solution (50 mM $NaPO_4$ buffer-30 mM Na_2HPO_4 + 20 mM NaH_2PO_4-, 2 mM potassium ferricyanide, 2mM potassium ferrocyanide, 0.05% Triton X-100, 1 mg mL^{-1} X-Gluc, pH 7). The incubation time varies according to the analyzed tissue: 30 min to 3 h for roots, 6 to 12 h for inflorescences and up to 24 h of coloration for rosettes, stem leaves and stems.

Protein localization analysis

A KUP9 protein fusion with the GFP reporter was generated to localize the KUP9 transporter. The coding sequence of *KUP9* was PCR amplified (forward primer:

ATGGCGGAAAGAGTCGAAGCATC, reverse primer: CTAAACATAAAAGACTTGTCCAACG) on Col-0 cDNA synthetized from 1 µg RNA with SuperScript™ III kit (Invitrogen). Sequencing of PCR products (GATC Biotech, Konstanz, Germany) reveals that the amplified fragments correspond to the splicing variant named At4g19960.2 in TAIR database (**Fig. 1**). This coding sequence was inserted into PCR-XL-TOPO optimizing this way its further insertion into the entry vector pDONR P2r-P3 (*att*B2r forward primer: *GGGGACAGCTTTCTTGTACAAAGTGG**TC***ATGGCGGAAAGAGTCGAAG, *att*B3 reverse primer: *GGGGACAACTTTGTATAATAAAGTTG**C***CTAAACATAAAAGACTTGTCCAACG) for cloning using Gateway® technology. One LR recombination was performed following the manufacturer's instructions to combine simultaneously pDONR P2r-P3 containing the *KUP9* CDS, pDONR221 containing *GFP* CDS, pDONRP4-P1r containing either the *35S* promoter or the *KUP9* native promoter and the destination vector pB7m34GW. Transgenic Arabidopsis plants carrying the resulting pro*35S*:*GFP-KUP9* and pro*KUP9*:*GFP-KUP9* constructs were obtained using the floral dip method (Clough and Bent 1998).

Transcriptional analysis of HAK5

For RT-qPCR analysis of *HAK5* expression, total RNA was extracted with the RNeasy kit (Qiagen, protocol for plants) from roots of 29-34 days-old plants, grown during 7 days in hydroponics with 10, 100 or 3000 µM K^+. The cDNA was synthesized from 1 µg of total RNA extracted on three biological replicates with SuperScript® Vilo™in 20 µL. Quantitative PCR was performed using the SYBR Green Master Mix on a Light Cycler 480 (Roche) with PCR amplification at 95°C for 10 s and 60°C for 10 s on three technical replicates. Relative expression of *HAK5* were calculated by normalization to the *ROC3* (At2g16600) gene expression (Arnaud et al. 2014, Ayadi et al. 2015, Bonnot et al. 2016). The primers for *ROC3* were TCGGTGAAAGCTTGATCCTT (forward) and ATCGTGATGGAGCTTTACGC (reverse); the primers for *HAK5* were ATCTAATGGGAGAGACCGAG (forward) and AACTCATAGGTCATGCCAAC (reverse). This experiment was performed on three independents bulks of plants.

Statistical analyses

ANOVA analyses were performed in the R environment (version 3.5.1) to evaluate the effects of the different treatments on plant K^+, Rb^+ and Cs^+ content and on root elongation separately (NS, Non-Significant and *, **, *** Significant at the α = 0.05, 0.01 and 0.001 level respectively). In tables,

different letters in bold indicate significant differences between means (Tuckey post-hoc test, *P*-value < 0.05).

As generally described for expression analyses using RT-qPCR (Yuan et al. 2006), statistical significances of fold-change in *HAK5* expression were tested applying Student *t*-test (unpaired data, one-tailed test) on Ct differences between the reference gene *ROC3* and the target gene *HAK5* in treated plants (supplied with 10 or 100 µM K^+) and in the control plants (supplied with 3000 µM K^+).

Results

KUP9 is preferentially expressed in roots and pollen and affected by K^+ supply

Reporter gene experiments were performed to determine the spatial expression pattern of *KUP9* in plants. Transgenic *Arabidopsis* lines expressing a GFP-GUS fusion protein under the control of the native *KUP9* promoter (pro*KUP*9:*GFP-GUS*) were generated. Following staining of different plant parts, GUS coloration was observed mainly in 7 days-old seedlings roots, in accordance with concomitant work (Zhang et al. 2020), but also in mature plant flowers (**Fig. 2**). In leaves, GUS coloration was not detected in most cases or was restricted to small areas often close to the base of trichomes.

In roots, GUS staining was notably stronger in seedlings growing in nutritive solution containing a low concentration of K^+ (**Fig. 2A**), suggesting that K^+ supply affects *KUP9* transcription in 7 days-old *Arabidopsis* seedlings. This result was confirmed by quantitative PCR, which indicated that *KUP9* expression is 1.4-fold higher (*P*-value 0.005) in Col-0 grown in low K^+ supply compared to sufficient K^+ condition (**Fig. S1**). Cross-section revealed that GUS staining was observed in all cell layers of the roots (**Fig. 2B**).

Performing RT-qPCR, *KUP9* mRNAs were detected in shoots of Col-0 (**Fig. S1**), while GUS coloration was not visible on leaves except in hydathodes even after 24h staining. This result could be due to the mobility of *KUP9* mRNA between roots and shoot (Thieme et al. 2015) or/and the existence of additional *KUP9* promoter sequences outside the 2745 bp fragment used in the proKUP9:GFP-GUS construction.

Localisation of the KUP9 transporter

Cellular localization of the KUP9 transporter was attempted generating transgenic *A. thaliana*, which expressed N-terminal GFP fusions with KUP9 transporter under the control of the 35S promoter (pro35S:GFP-KUP9) or under the control of the KUP9 promoter (proKUP9:GFP-KUP9). The current

KUP9 gene model implies four distinct transcripts (The Arabidopsis Information Resource, TAIR, www.arabidopsis.org/servlets/TairObject?id=127288&type=locus, on www.arabidopsis.org, May 07, 2020). Sequencing of the PCR products from *KUP9* cDNA in Col-0 used for these constructions corresponded to the splicing variant named At4g19960.2 in the TAIR database.

Unfortunately, even though no errors were detected in sequencing, these constructions led to the synthesis of a cleaved protein (37 kDa protein detected in western blot, **Appendix S2** and **Fig. S2**), and we were not able to detect GFP signals in transgenic lines. In a recent work, Zhang et al. (2020), however, localized the KUP9 transporter from the At4g19960.3 splice variant (according to the TAIR 10 database) mainly in the endoplasmic reticulum.

Predicted proteins from the four *KUP9* splice variants differ in their amino acid sequences length (**Fig.1**). Different isoforms of a protein can have distinct functions or localization (Brummell et al. 2011, Kriechbaumer et al. 2012, reviewed in Syed et al. 2012). However, deeper analyses are needed to establish the prevalence of each splicing variant (which can depend on tissue, developmental stage or environmental stresses, Syed et al. 2012) or the impact of splicing choice on protein function.

kup9 mutants do not display defective K^+ content

Several members of the *KUP/HAK/KT* family have already been shown to be involved in K^+ transport in *A. thaliana*. Expressed in an *Escherichia coli* mutant strain that lacks its three major K^+ uptake systems, AtKUP9 likely mediates K^+ influx (Kobayashi et al. 2010). Endoplasmic reticulum-localized KUP9 participates in maintaining meristem activity under low K^+ conditions, likely mediating local K^+ and auxin efflux toward the cytoplasm of quiescent center cells (Zhang et al. 2020). To further understand its role in the overall plant K^+ homeostasis, *kup9* Arabidopsis mutant lines were compared to wild-type plants for their K^+ status under three different levels of K^+ supply (**Fig. 3**).

Under low (10 µM) and sufficient (3000 µM) K^+ supply, shoot K^+ content tended to be higher in *kup9* mutant lines compared to Col-0, whereas K^+ content in roots was nearly the same for the three lines in all tested levels of K^+ supply. In addition, there were no significant differences for Rb^+ (used as a K^+ tracer) influx in plants lacking *KUP9* compared to wild-type (**Table 1**). Taking together these results suggest that, in our conditions (30 days-old plants grown in nutrient solution containing 10, 100 or 3000 µM K^+ for 7 days), disruption of *KUP9* does not result in a significant decrease of the shoot and root K^+ content.

kup9 mutants are more sensitive to Cs^+

Based on a previous work showing that a K^+ transport-deficient *E. coli* mutant expressing *AtKUP9* was able to take up Cs^+ (Kobayashi et al. 2010), we wondered whether *kup9* Arabidopsis mutants differed from wild-type in their response to Cs^+. Cotyledon development and primary root elongation of wild-type and of the two mutant lines disrupted in *AtKUP9* were compared on media containing low (10 µM) or high (1000 µM) levels of K^+ and a range of Cs^+ concentrations (**Fig. 4**). A mutant lacking *AtHAK5* previously screened in similar experiments (Qi et al. 2008) was used to validate our conditions.

Cotyledons of seedlings grown in liquid media were bleached in the presence of toxic concentrations of Cs^+ (**Fig. 4A**). Conversely, to plants grown in media containing 1000 µM K^+, the different lines displayed different sensitivities to Cs^+ when grown in 10 µM K^+. For *kup9* mutant lines supplied with a low amount of K^+, bleaching occurred at 10 µM of Cs^+ whereas cotyledons of wild-type remained green. Increasing the concentrations of Cs^+ (100 µM) bleached the cotyledons of the wild-type completely, whereas those of *hak5-3* remain partly green.

In vertical plates containing a low amount of K^+ (14-40 µM, measured in ICP-AES), primary root elongation of both *kup9* mutant lines was significantly lower than those of wild-type plants when Cs^+ concentration reached 100 µM (**Fig. 4.B**). Thus, plants lacking *KUP9* appeared more sensitive to Cs^+ when grown under low K^+-supply. Conversely, *HAK5* disruption enhanced Cs^+ tolerance under the same conditions, which is consistent with its role in Cs^+ uptake. Discrepancies in Cs^+ toxicity between the different lines were not visible in plants grown in higher amounts of K^+ (1000 µM).

In recent works, Zhang et al. (2020) observed an inhibition of the primary root growth in *kup9* mutants under low K^+ conditions (50 µM). Here, we did not measure statistical differences in primary root elongation between lines in the absence of Cs^+ may be due to the growth of the seedlings in MS½ prior to the experiment.

kup9 mutants accumulate more Cs^+

Cs^+ toxicity in plants may originate from K^+ starvation caused by the presence of Cs^+ in the rhizosphere (Maathuis and Sanders 1996) and is related to the Cs^+:K^+ concentration ratio at the tissue level (Hampton et al. 2004). Since *KUP9* disruption does not negatively alter the K^+ status but does increase sensitivity to Cs^+, we wondered whether it affects Cs^+ accumulation in plants. Cs^+ content was compared in Col-0 wild-type and *kup9* mutant lines exposed to 1 µM CsCl for 7 days in hydroponics conditions (**Fig. 5A**). A *hak5* mutant line was also used as control in our experiments. In plants grown with sufficient K^+ supply (3000 µM), disruption of *KUP9* and *HAK5* had no significant effect on Cs^+ accumulation. When K^+ supply was low (10 µM), Cs^+ accumulation increased to different extent depending on the plant line. As expected under low K^+ supply, plants lacking *HAK5* accumulated 50%

less of Cs^+ than the wild-type. Under the same condition, disruption of *KUP9* had the opposite effect resulting in a higher accumulation of Cs^+ than the wild-type (around 30% more). This is consistent with a recently published experiment performed in liquid media containing 500 µM K^+ and 300 µM Cs^+ showing that *kup9-1* seedlings accumulate more Cs^+ than the wild-type Col-0 (Adams et al. 2019).

Examining shoot and roots Cs^+ contents separately (**Table 2**), it appeared that Cs^+ distribution remained globally unchanged in *kup9* mutant lines compared to wild-type. Interestingly, when K^+-supply was low (10 µM), *hak5-3* mutants displayed a divergent pattern of Cs^+ distribution with a lower Cs^+ Root:Shoot concentration ratio. This was due to a significant decrease of Cs^+ concentrations in roots (50.7 ± 11.8 and 14.9 ± 3.5 µmol g^{-1} DW in Col-0 and *hak5-3*, respectively) whereas concentrations in shoots remained unchanged (4 ± 0.5 and 3.9 ± 0.4 µmol g^{-1} DW in Col-0 and *hak5-3*, respectively). Role of HAK5 in roots Cs^+ uptake (Qi et al. 2008) and the recent model excluding HAK5 in K^+ translocation in low K^+ plants (Nieves-Cordones et al. 2019) may provide valuable leads to explain the particular Cs^+ distribution pattern observed in *hak5-3*.

To further investigate mechanisms leading to an increase of Cs^+ accumulation in plants lacking *KUP9*, fluxes of Cs^+ between roots and the external medium were measured in wild-type and in *kup9* mutant lines (**Fig. 5B**). First, K^+-starved plants were exposed to a K^+-free solution containing Cs^+. In 24 h, the amount of Cs^+ in this solution decreased by 74 to 85% in *kup9* mutant lines, whereas only 30% was taken up by wild-type plants. The differences between the lines appeared over the first three hours but are not clearly displayed during the first hour, suggesting that KUP9 may participate in Cs^+ transport mechanisms that require time to be significant at the whole scale level. Contaminated plants were then transferred in a Cs^+-free solution in which Cs^+ release was followed. Significant amount of Cs^+ was detected in the external medium from the first hour, suggesting that Cs^+ is quickly released by plants. After 24 h, the initially Cs^+-free solution contained 2.71 µM (± 0.57), 4.07 µM (± 0.39) and 3.47 µM (± 1.15) of Cs^+ for Col-0, *kup9-3* and *kup9-1* respectively. Interestingly, it was noticed that *kup9* lines released less Cs^+ than wild-type in proportion when the amount of Cs^+ released in the solution was normalized by the amount of Cs^+ accumulated in plants at the beginning of the experiment.

Discussion

KUP9 prevents Cs^+ accumulation in plants

Cs^+ accumulation in plants depends on the level of K^+-supply, and several K^+ transporters have been shown to mediate opportunistic Cs^+ fluxes (**Fig. 6**). The contributions of HAK5 (Qi et al. 2008, Nieves-Cordones et al. 2020) and NSCC (White and Broadley 2000, Hampton et al. 2005) to Cs^+ uptake in roots and the role of ZIFL2 in regulating xylem Cs^+ content (Remy et al. 2015) allowed the

unravelling of the molecular identity of proteins involved in Cs^+ transport. Recently, ABCG33 and ABCG37, two ABC proteins, have been shown to mediate redundantly potassium-independent Cs^+ influx in Arabidopsis roots (Ashraf et al. 2021). In contrast, transporters mediating Cs^+ translocation from the roots and the shoot remain unclear. In this way, further investigations are needed to determine the roles of transport systems involved in K^+ translocation such as the stellar K^+ outward-rectifying channel SKOR (Gaymard et al. 1998, Drechsler et al. 2015), the nitrate transporter1/peptide transporter NRT1.5 (Drechsler et al. 2015, Li et al. 2017), the K^+ transporters KUP7 (Han et al. 2016) and HAK5 (Nieves-Cordones et al. 2019) for instance. Identities of carriers involved in Cs^+ transport from the cytosol to the organelles and also mechanisms underlying Cs^+ release from root cells to the external medium remain unknown as well. In the present study, analysis of *kup9* mutant lines provides several points of evidence involving KUP9 transporter in the limitation of Cs^+ accumulation under low K^+-supply condition in *A. thaliana*.

First, *kup9* mutant lines display higher sensitivity to Cs^+ which is reflected by cotyledons bleaching and reduced root elongation for lower Cs^+ concentrations compared with wild-type. When used in the millimolar range, Cs^+ is toxic and induces a K^+ decrease in shoots (Hampton et al. 2004). In our conditions, micromolar Cs^+ concentrations were sufficient to point out the higher sensitivity to Cs^+ in *kup9* mutant lines, and we did not measure a significant decrease in the K^+ status in the shoot of Cs^+-treated plants under these conditions (**Fig.S3**). Higher toxicity of Cs^+ in *kup9* mutant lines is therefore likely linked to the toxicity of Cs^+ itself rather than to a concomitant alteration of K^+ status in shoots. This is supported by the second point showing the role of KUP9 in Cs^+ transport, which is the higher accumulation of Cs^+ in *kup9* mutant lines. Conversely, to the results showing that *AtKUP9* mediates Cs^+ uptake when expressed in *E. coli* mutants (Kobayashi et al. 2010), our results demonstrate that *KUP9* is not directly involved in Cs^+ influx in roots of *A. thaliana* but participates in limiting Cs^+ accumulation in plants. Such discrepancies between heterologous and *in planta* analyses have been already addressed and attributed to, for example, artificial interactions with heterologous structures or to the lack of regulatory proteins from the native organism (Dreyer et al. 1999).

The level of K^+-supply has a major effect on Cs^+ accumulation in plants. This is linked to several factors, such as the competition between the two cations for the same transport systems and the control of transporter expression by K^+-supply. In our study, *kup9* mutants displayed enhanced Cs^+ accumulation only when supplied with a low level of K^+. We suggest that, at sufficient K^+-supply (mM range), the relative lower transcription of *KUP9* in wild-type plants and the higher external Cs^+ dilution may contribute to blur the discrepancies between *kup9* and wild-type Cs^+ accumulation. Besides regulations occurring at the transcriptional level, post-translational modifications and, in particular, phosphorylation have also been reported in regulation of high-affinity K^+ uptake through HAK5 (Ragel et al. 2015) and in KUP7 activity (Han et al. 2016). Querying database for phosphorylation sites in plants (dbPPT, Cheng et al. 2014), did not results in any hits for the KUP9

transporter. Computational predictions (Musite, Yao et al. 2012), applied on the KUP9 peptide sequence, pointed out at least one phosphorylation site with high specificity (> 95%). It would be interesting to further investigate these putative phosphorylation sites and their contribution to KUP9 activation under different K^+ conditions.

Role of KUP9 in Cs^+ transport

In the present study, we have shown that Cs^+ release from roots to the external solution is proportionally two times lower in plants lacking KUP9 compared with wild-type (**Fig. 5**). Given this indirect evidence, it is tempting to speculate that KUP9 could work as an efflux carrier permeable to Cs^+:

(1) either from an organelle to the cytosol (*HYP. A* in **Fig. 6**). In that case, disruption of KUP9 may encourage cations sequestration into organelles, and the decrease of cations into the cytosol may, in turn, encourage cations influx from the external medium. The concomitant work of Zhang et al. (2020), reporting K^+ efflux through KUP9 expressed in heterologous systems and localizing KUP9 transporter in the endoplasmic reticulum, provides important leads in favor of this hypothesis.

(2) or from the cytosol to the apoplasm of root cells before release in the external medium (*HYP. B* in **Fig. 6**). This is supported by similar results suggesting that the KUP6 sub-family, i.e. KUP6, KUP8 and KUP2 (**Fig. 7**), may participate with the Shaker channel GORK in the efflux of K^+ from roots during K^+ starvation (Osakabe et al. 2013). Based on thermodynamical considerations (Rodríguez-Navarro 2000), experiments on HAK-like activity in salt bladders of a halophyte plant species (Böhm et al. 2018) and electrophysiologic analyses (Scherzer et al. 2015, Nieves-Cordones et al. 2017), it is highly probable that KUP transporters operate as K^+-H^+ symporters (Ragel et al. 2019). Therefore, to test directly whether the KUP9 transporter is involved in Cs^+ efflux from the roots to the external solution, future work comparing Cs^+ release for different pH gradients across the plasma membrane between Col-0 and *kup9* mutants should be done.

Alternative hypothesis (*HYP. C* in **Fig. 6**) involving compensatory mechanisms should also be tested in future work: the potential KUP9-mediated part of plant K^+ uptake could be supported by other K^+ transporters, more or less permeable to Cs^+, in *kup9* mutant lines. In this context, we wondered whether overactivation of HAK5 could compensate for the part of KUP9-mediated K^+ uptake in *kup9* mutant lines, leading to an overaccumulation of Cs^+ due to HAK5- mediated Cs^+ uptake at the same time. Preliminary results indicate that *HAK5* is induced from a less low K^+ concentration in *kup9* mutants but, no differences were detected at 10 µM K^+ (**Table 3**). Further experiments testing whether *hak5kup9* double mutants accumulate more Cs^+ than the *hak5* single mutants, for instance, are needed

to conclude about the role that HAK5 might have in the mechanisms potentially involved in compensating for the absence of KUP9.

Primary plant role of KUP9

Cs^+ has no relevant functions in plants suggesting that transport of Cs^+ through KUP9 transporter is more probably a non-specific process. In *A. thaliana*, KUP9 belongs to the KUP/HAK/KT family organized in 4 clades (**Fig. 7**), and the other KUP transporters have been related to various biological processes such as roots K^+ acquisition (HAK5, Rubio et al. 2000, Gierth et al. 2005) and translocation (KUP7, Han et al. 2016), growth and development (KUP4, Rigas et al. 2001; KUP2, Elumalai et al. 2002; KUP6 and KUP8, Osakabe et al. 2013) or responses to heavy metal (KUP8, Sanz-Fernández et al. 2021). In *E. coli* mutants defective in the constitutive K^+ transport systems, heterologous expression of *AtKUP9* is able to mediate K^+ uptake (Kobayashi et al. 2010). It is worth noting that KUP9 has recently been shown to contribute to auxin and K^+ homeostasis in quiescent center cells in low K^+ conditions, thereby maintaining root meristem activity and root growth in *A. thaliana* (Zhang et al. 2020). In other plant species, such as the extremophytes *Schrenkiella parvula*, *A. lyrata* and *A. arenosa*, it is thought that higher expression strength and single-nucleotide polymorphism affecting *KUP9* homologs might be related to an adjustment in K^+ transport supporting plants adaptation to soils containing challenging ions concentrations (Turner et al. 2010, Oh et al. 2014, Arnold et al. 2016). For *A. thaliana* tested under experimental conditions described here, however, we did not detect significant effects of *KUP9* disruption in the overall plant K^+ homeostasis. On the contrary to Cs^+, K^+ is involved in many biological processes, and K^+ homeostasis is tightly regulated. Therefore, we assumed that compensatory mechanisms through redundant functions of K^+ carriers could be induced in the tested *kup9* mutant lines blurring potential discrepancies with wild-type plants

The primary plant role of KUP9 could also be significant in other plant stages not tested in this study. Indeed, the activity of GUS reporter in transgenic plants carrying the Pro*KUP*9:*GFP-GUS* construct reveals expression of *KUP9* in certain pollen grains (**Fig. 2D**). This is consistent with previous transcriptome analyses showing the late pollen-expression pattern of *KUP9*, which differs from the other *KUP* on this point (Bock et al. 2006). The functions of potassium transporters are crucial for pollen tube growth (Mouline et al. 2002). For example, SlHAK5 has been recently shown to be involved in K^+ accumulation in pollen grains and to contribute to pollen viability (Nieves-Cordones et al. 2020). Therefore, it could be interesting to further investigate the role of KUP9 in pollen development

Phytoremediation strategies to manage Cs^+-contaminated soils

The use of plants for remediation of radiocesium-contaminated soils as well as the development of "safe crops" receive considerable interest for a few decades (Zhu and Shaw 2000, White et al. 2003). However, the fact that Cs^+ enters plants through the K^+ transport system is a major constraint for phytoremediation strategies. Controlling the expression of major potassium transporters, such as HAK5, to increase/decrease plant Cs^+ acquisition without disturbing K^+ nutrition may imply modulating their specificity (Alemán et al. 2014). By contrast, the two *kup9* mutant lines tested in the present study display higher Cs^+ accumulation without significant alteration of K^+ status when supplied with a low level of K^+. We proposed that KUP9 may prevent Cs^+ accumulation by releasing it from root cells and that the potential role of KUP9 in K^+ homeostasis appears to be minor in the experimental conditions used here. Manipulating expression of such minor K^+ transporters, whose disruption does not alter plant K^+ acquisition but does enhance substantially Cs^+ accumulation, may offer a valuable alternative for phytoremediation strategies.

Author contributions

N.L., A.V. and P.H. designed the research; L.G., L.M., S.K., S.C., L.C., and V.C. performed the research; L.G., N.L. and P.H. analyzed the data and wrote the paper.

Acknowledgements

This work, conducted under the DEMETERRES project, was supported by the National Research Agency (ANR-11-RSNR-005).

References

Adams E, Miyazaki T, Shin R (2019) Contribution of KUPs to potassium and cesium accumulation appears complementary in *Arabidopsis*. Plant Signal Behav 14: e1554468

Akamatsu M, Komatsu H, Mori T, Adams E, Shin R, Sakai H, Abe M, Hill JP, Ariga K (2014) Intracellular Imaging of Cesium Distribution in *Arabidopsis* Using Cesium Green. ACS Appl Mater Inter 6: 8208-8211

Alemán F, Nieves-Cordones M, Martínez V, Rubio F (2011) Root K^+ acquisition in plants: the *Arabidopsis thaliana* model. Plant Cell Physiol 52: 1603-1612

Alemán F, Caballero F, Ródenas R, Rivero RM, Martínez V, Rubio F (2014) The F130S point mutation in the Arabidopsis high-affinity K^+ transporter AtHAK5 increases K^+ over Na^+ and Cs^+

selectivity and confers Na^+ and Cs^+ tolerance to yeast under heterologous expression. Front Plant Sci 5: 430

Arnaud C, Clément M, Thibaud MC, Javot H, Chiarenza S, Delannoy E, Revol J, Soreau P, Balzergue S, Block MA, Maréchal E, Desnos T, Nussaume L (2014) Identification of phosphatin, a drug alleviating phosphate starvation responses in Arabidopsis. Plant Physiol 2014 166(3):1479-1491

Arnold BJ, Lahner B, DaCosta JM, Weisman CM, Hollister JD, Salt DE, Bomlies K, Yant L (2016) Borrowed alleles and convergence in serpentine adaptation. Proc Natl Acad Sci USA 113: 8320-8325

Ashraf MA, Akihiro T., Ito K, Kumagai S, Sugita R, Tanoi K, Rahman A (2021) ATP binding cassette proteins ABCG37 and ABCG33 function as potassium-independent cesium uptake carriers in *Arabidopsis* roots. Mol Plant 14: 1-15

Ayadi A, David P, Arrighi JF, Chiarenza S, Thibaud MC, Nussaume L, Marin E (2015) Reducing the genetic redundancy of Arabidopsis PHOSPHATE TRANSPORTER1 transporters to study phosphate uptake and signaling. Plant Physiol 167(4):1511-1526

Bange G, Overstreet R (1960) Some observations on absorption of cesium by excised barley roots. Plant Physiol 35: 605-608

Bertl A, Reid JD, Sentenac H, Slayman CL (1997) Functional comparison of plant inward-rectifier channels expressed in yeast. J Exp Bot 48: 405-413

Böhm J, Messerer M, Müller HM, Scholz-Starke J, Gradogna A, Scherzer S, Maierhofer T, Bazihizina N, Zhang H, Stigloher C, Ache P, Al-Rasheid KAS, Mayer KFX, Shabala S, Carpaneto A, Haberer G, Zhu JK, Hedrich R (2018) Understanding the molecular basis of salt sequestration in epidermal bladder cells of *Chenopodium quinoa*. Curr Biol 28: 3075–3085

Bock KW, Honys D, Ward JM, Padmanaban S, Nawrocki EP, Hirschi KD, Twell D, Sze H (2006) Integrating membrane transport with male gametophyte development and function through transcriptomics. Plant Physiol 140: 1151-1168

Bonnot C, Pinson B, Clément M, Bernillon S, Chiarenza S, Kanno S, Kobayashi N, Delannoy E, Nakanishi TM, Nussaume L, Desnos T (2016) A chemical genetic strategy identify the PHOSTIN, a synthetic molecule that triggers phosphate starvation responses in *Arabidopsis thaliana*. New Phytol 209: 161-176

Bossemeyer D, Schlösser A, Bakker EP (1989) Specific cesium transport via the *Escherichia coli* Kup (TrkD) K^+ uptake system. J Bacteriol 171: 2219-2221

Bowen HJM (1979) Environmental chemistry of the elements. Academic Press, London

Broadley MR, Escobar-Gutiérrez AJ, Bowen HC, Willey NJ, White PJ (2001) Influx and accumulation of Cs^+ by the *akt1* mutant of *Arabidopsis thaliana* (L.) Heynh. lacking a dominant K^+ transport system. J Exp Bot 52: 839-844

Brummell DA, Chen RKY, Harris JC, Zhang H, Hamiaux C, Kralicek AV, McKenzie MJ (2011) Induction of vacuolar invertase inhibitor mRNA in potato tubers contributes to cold-induced sweetening resistance and includes spliced hybrid mRNA variants. J Exp Bot 62 : 3519-3534

Cheng H, Deng W, Wang Y, Ren J, Liu Z, Xue Y (2014) dbPPT: a comprehensive database of protein phosphorylation in plants. Database 2014: 1-8

Clough SJ, Bent AF (1998) Floral dip: A simplified method for *Agrobacterium*-mediated transformation of *Arabidopsis thaliana*. Plant J 16: 735-743

Collander R (1941) Selective absorption of cations by higher plants. Plant Physiol 16: 691-720

Dreyer I, Horeau C, Lemaillet G, Zimmermann S, Bush DR, Rodríguez-Navarro A, Schachtman DP, Splading EP, Sentenac H, Gaber RF (1999) Identification and characterization of plant transporters using heterologous expression systems. J Exp Bot 50: 1073-1087

Drechsler N, Zheng Y, Bohner A, Nobmann B, von Wirén N, Kunze R, Rausch C (2015) Nitrate-dependent control of shoot K homeostasis by NPF7.3/NRT1.5 and SKOR in Arabidopsis. Plant Physiol 169: 2832–2847

Elumalai RP, Nagpal P, Reed JW (2002) A mutation in the *Arabidopsis KT2/KUP2* potassium transporter gene affects shoot cell expansion. Plant Cell 14: 119-131

Epstein E, Hagen C (1952) A kinetic study of the absorption of alkali cations by barley roots. Plant Physiol 27: 457-474

Gaymard F, Pilot G, Lacombe B, Bouchez D, Bruneau D, Boucherez J, Michaux-Ferrière N, Thibaud JB, Sentenac H (1998) Identification and disruption of a plant shaker-like outward channel involved in K^+ release into the xylem sap. Cell 94: 647–655

Genies L, Orjollet D, Carasco L, Camilleri V, Frelon S, Vavasseur A, Leonhardt N, Henner P (2017) Uptake and translocation of cesium by *Arabidopsis thaliana* in hydroponics conditions: Links between kinetics and molecular mechanisms. Environ Exp Bot 138: 164-172

Gierth M, Mäser P, Schroeder JI (2005) The potassium transporter AtHAK5 functions in K^+ deprivation-induced high-affinity K^+ uptake and AKT1 K^+ channel contribution to K^+ uptake kinetics in *Arabidopsis* roots. Plant Physiol 137: 1105-1114

Greenwood NN, Earnshaw A (1997) Chemistry of the Elements, 2nd Edn. Butterworth-Heinemann, pp 68-106

Hamada N, Ogino H (2012) Food safety regulations: what we learned from the Fukushima nuclear accident. J Environ Radioact 111: 83-99

Hampton CR, Bowen HC, Broadley MR, Hammond JP, Mead A, Payne KA, Pritchard J, White PJ (2004) Cesium toxicity in Arabidopsis. Plant Physiol 136: 3824-3837

Hampton, C.R., Broadley, M.R. and White P.J. (2005) Short review: the mechanisms of radiocaesium uptake by *Arabidopsis* roots. Nukleonika 50: 3-8

Han M, Wu W, Wu WH, Wang Y (2016) Potassium Transporter KUP7 Is Involved in K^+ Acquisition and Translocation in *Arabidopsis* Root under K^+-Limited Conditions. Mol Plant 9: 437-446

Hirsch RE, Lewis BD, Spalding EP, Sussman MR (1998) A role for the AKT1 potassium channel in plant nutrition. Science 280: 918-921

Kobayashi D, Uozumi N, Hisamatsu S, Yamagami M (2010) AtKUP/HAK/KT9, a K^+ transporter from *Arabidopsis thaliana*, mediates Cs^+ uptake in *Escherichia coli*. Biosci Biotech and Bioch 74: 203-205

Kondo M, Makino T, Eguchi T, Goto A, Nakano H, Takai T, Arai-Sanoh Y, Kimura T (2015) Comparative analysis of the relationship between Cs and K in soil and plant parts toward control of Cs accumulation in rice. Soil Sci Plant Nutr 61: 144-151

Kriechbaumer V, Wang P, Hawes C, Abell BM (2012) Alternative splicing of the auxin biosynthesis gene *YUCCA4* determines its subcellular compartmentation. Plant J 70: 292-302

Le Lay P, Isaure MP, Sarry JE, Kuhn L, Fayard B, Le Bail JL, Bastien O, Garin J, Roby C, Bourguignon J (2006) Metabolomic, proteomic and biophysical analyses of *Arabidopsis thaliana* cells exposed to a caesium stress. Influence of potassium supply. Biochimie 88: 1533-1547

Li H, Yu M, Du XQ, Wang ZF, Wu WH, Quintero FJ, Jin XH, Li HD, Wang Y (2017) NRT1.5/NPF7.3 functions as a proton-coupled H^+/K^+ antiporter for K^+ loading into the xylem in *Arabidopsis*. Plant Cell 29: 2016–2026

Maathuis FJ, Sanders D (1996) Characterization of *csi52*, a Cs^+ resistant mutant of *Arabidopsis thaliana* altered in K^+ transport. Plant J 10: 579-589

Mäser P, Thomine S, Schroeder JI, Ward JM, Hirschi K, Sze H, Talke IN, Amtmann A, Maathuis FJM, Sanders D, Harper JF, Tchieu J, Gribskov M, Persans MW, Salt DE, Kim SA, Guerinot ML

(2001) Phylogenetic relationships within cation transporter families of *Arabidopsis*. Plant Physiol 126: 1646-1667

Middleton LJ, Handley R, Overstreet R (1960) Relative uptake and translocation of potassium and cesium in barley. Plant Physiol 35: 913-918

Mouline K, Véry AA, Gaymard F, Boucherez J, Pilot G, Devic M, Bouchez D, Thibaud JB, Sentenac H (2002) Pollen tube development and competitive ability are impaired by disruption of a Shaker K^+ channel in *Arabidopsis*. Genes Dev 16: 339-350

Murashige T, Skoog F (1962) A revised medium for rapid growth and bio assays with tobacco tissue cultures. Physiol Plant 15: 473-497

Nieves-Cordones M, Mohamed S, Tanoi K, Kobayashi NI, Takagi K, Vernet A, Guiderdoni E, Périn C, Sentenac H, Véry AA (2017) Production of low-Cs^+ rice plants by inactivation of the K^+ transporter OsHAK1 with the CRISPR-Cas system. Plant J 92: 43–56

Nieves-Cordones M, Lara A, Ródenas R, Amo J, Rivero RM, Martínez V, Rubio F (2019) Modulation of K^+ translocation by AKT1 and AtHAK5 in *Arabidopsis* plants. Plant Cell Environ 42: 2357-2371

Nieves-Cordones M, Lara A, Silva M, Amo J, Rodriguez-Sepulveda P, Rivero RM, Martínez V, Botella MA, Rubio F (2020) Root hight-affinity K^+ and Cs^+ uptake and plant fertility in tomato plants are dependent on the activity of the high-affinity K^+ transporter SIHAK5. Plant Cell Environ 43: 1707-1721

Oh DH, Hong H, Lee SY, Yun DJ, Bohnert HJ, Dassanayake M (2014) Genome structures and transcriptomes signify niche adaptation for the multiple-ion-tolerant extremophyte *Schrenkiella parvula*. Plant Physiol 164: 2123-2138

Osakabe Y, Arinaga N, Umezawa T, Katsura S, Nagamachi K, Tanaka H, Ohiraki H, Yamada K, Seo SU, Abo M, Yoshimura E, Shinozaki K, Yamaguchi-Shinozaki K (2013) Osmotic stress responses and plant growth controlled by potassium transporters in *Arabidopsis*. Plant Cell 25: 609-624

Qi Z, Hampton CR, Shin R, Barkla BJ, White PJ, Schachtman DP (2008) The high affinity K^+ transporter AtHAK5 plays a physiological role in planta at very low K^+ concentrations and provides a caesium uptake pathway in *Arabidopsis*. J Exp Bot 59: 595-607

Ragel P, Ródenas R, García-Martín E, Andrés Z, Villalta I, Nieves-Cordones M, Rivero RM, Martínez V, Pardo JM, Quintero FJ, Rubio F (2015) The CBL-interacting protein kinase CIPK23 regulates HAK5-mediated high-affinity K^+ uptake in *Arabidopsis* roots. Plant Physiol 169: 2863-2873

Ragel P, Raddatz N, Leidi EO, Quintero FJ, Pardo JM (2019) Regulation of K^+ nutrition in plants. Front Plant Sci 10: 281

Remy E, Cabrito, TR, Batista RA, Teixeira MC, Sa-Correia I, Duque P (2015) The Major Facilitator Superfamily Transporter ZIFL2 Modulates Cesium and Potassium Homeostasis in *Arabidopsis*. Plant Cell Physiol 56: 148-162

Rigas S, Debrosses G, Haralampidis K, Vicente-Agullo F, Feldmann KA, Grabov A, Dolan L, Hatzopoulos P (2001) *TRH1* encodes a potassium transporter required for tip growth in *Arabidopsis* root hairs. Plant Cell 13: 139-151

Rodríguez-Navarro A (2000) Potassium transport in fungi and plants. Biochim Biophys Acta 1469: 1-30

Rubio F, Santa-María GE, Rodríguez-Navarro A (2000) Cloning of *Arabidopsis* and barley cDNAs encoding HAK potassium transporters in root and shoot cells. Physiol Plant 109: 34-43

Rubio F, Nieves-Cordones M, Alemán F, Martínez V (2008) Relative contribution of AtHAK5 and AtAKT1 to K^+ uptake in the high-affinity range of concentrations. Physiol Plant 134: 598-608

Sacchi GA, Espen L, Nocito F, Cocucci M (1997) Cs^+ uptake in subapical maize root segments: Mechanism and effects on H^+ release, transmembrane electric potential and cell pH. Plant Cell Physiol 38: 282-289

Sanz-Fernández M, Rodríguez-González A, Sandalio LM, Romero-Puertas MC (2021) Role of potassium transporter KUP8 in plant responses to heavy metals. Physiol Plant 1-11

Scherzer S, Böhm J, Krol E, Shabala L, Kreuzer I, Larisch C, Bemm F, Al-Rasheid KAS, Shabala S, Rennenberg H, Neher E, Hedrich R (2015) Calcium sensor kinase activates potassium uptake systems in gland cells of *Venus flytraps*. Proc Natl Acad Sci USA 112: 7309–7314

Shaw G, Bell J (1989) The kinetics of caesium absorption by roots of winter wheat and the possible consequences for the derivation of soil-to-plant transfer factors for radiocaesium. J Environ Radioact 10: 213-231

Smolders E, Kiebooms L, Buysse J, Merckx R (1996) 137Cs uptake in spring wheat (*Triticum aestivum* L. cv. Tonic) at varying K supply. Plant Soil 181: 211-220

Steinhauser G, Brandl A, Johnson TE (2014) Comparison of the Chernobyl and Fukushima nuclear accidents: A review of the environmental impacts. Sci Total Environ 470: 800-817

Syed NH, Kalyna M, Marquez Y, Barta A, Brown JWS (2012) Alternative splicing in plants – coming of age. Trends Plant Sci 17: 616-623

Tenorio-Berrío R, Pérez-Alonso MM, Vicente-Carbajosa J, Martín-Torres L, Dreyer I, Pollmann S (2018) Identification of two auxin-regulated potassium transporters involved in seed maturation. Int J Mol Sci 19: 2132

Thieme CJ, Rojas-Triana M, Stecyk E, Schudoma C, Zhang W, Yang L, Miñambres M, Walther D, Schulze WX, Paz-Ares J, Scheible WR, Kragler F (2015) Endogenous *Arabidopsis* messenger RNAs transported to distant tissues. Nat Plants 1(4) :15025

Turner TL, Bourne EC, Von Wettberg EJ, Hu TT, Nuzhdin SV (2010) Population resequencing reveals local adaptation of *Arabidopsis lyrata* to serpentine soils. Nat Genet 42: 260-263

White PJ, Broadley MR (2000) Tansley Review No. 113. Mechanisms of caesium uptake by plants. New Phytol 147: 241-256

White PJ, Swarup K, Escobar-Gutiérrez AJ, Bowen HC, Willey NJ, Broadley MR (2003) Selecting plants to minimise radiocaesium in the food chain. Plant Soil 249: 177-186

Yao Q, Gao J, Bollinger C, Thelen JJ, Xu D (2012) Predicting and analyzing protein phosphorylation sites in plants using Musite. Front Plant Sci 3: 186

Yuan JS, Reed A, Chen F, Stewart CN (2006) Statistical analysis of real-time PCR data. BMC Bioinform 7: 85

Zhang ML, Huang PP, Ji Y, Wang S, Wang SS, Li Z, Guo Y, Ding Z, Wu WH, Wang Y (2020) KUP9 maintains root meristem activity by regulating K^+ and auxin homeostasis in response to low K. EMBO Rep e50164

Zhu YG, Shaw G (2000) Soil contamination with radionuclides and potential remediation. Chemosphere 41: 121-128

Supporting information

Additional supporting information may be found online in the Supporting Information section at the end of the article:

Fig. S1. *KUP9* relative expression measured in RT-qPCR.

Appendix S2. Localisation of KUP9 transporter

Fig.S2. Check of pro*35S*:*GFP-KUP9* and pro*KUP9*:*GFP-KUP9* constructs in transgenic lines.

Fig. S3. K^+ content in Cs^+-exposed plants.

Table S1. List of primers.

Table S2. Cs^+ concentrations (µmol.g^{-1} dry weight) in shoots and roots of 30 days-old *Arabidopsis thaliana* plants exposed during 7 days to a nutrient solution containing 1 µM Cs^+ and 10 µM or 3000 µM K^+. Data are means ± SD (*n* =6-8).

Table S3. Adjusted *P*-values from Tukey HSD post-test for Cs^+ depletion assay presented in Figure 5.B1.

Data availability statement

The data that support the findings of this study are available from the corresponding authors upon reasonable request.

Figure legends

Figure 1: *KUP9* gene model and T-DNA insertion sites in *kup9-1* (SALK_108080C) and *kup9-3* (SAIL_211_E04) mutant lines. White boxes represent exons whereas dark lines between boxes denote introns of *AtKUP9* gene; light grey boxes represent 3' and 5'-UTR. The current *KUP9* gene model implies four distinct splice variants (The Arabidopsis Information Resource, TAIR, www.arabidopsis.org/servlets/TairObject?id=127288&type=locus, on www.arabidopsis.org, May 07, 2020). Dark grey boxes highlight changes between the different splicing variants (for the AT4g19960.4 model, the absence of amino acids at the beginning of the predicted protein is marked with a cross). For *kup9* mutant lines, T-DNA insertions are outlined by large triangle and black arrows represent gene specific primers used for mutant lines checking (F1: GGAGATTTAGGGACGTCTCCATTGTATGTG, R1: TCCTCATCACTACGGTGCTGATTCG; F2: CCTACAGCAGCACGTATTCCGTCAAC, R2: CGGTGTTCCCCATTATATGAACAACACCTG).

Figure 2: Spatial transcription pattern of *KUP9* determined in *ProKUP9:GFP-GUS* transgenic *A. thaliana* plants. GUS staining of (**A**) Roots of 7 days-old seedlings grown in nutritive agar medium with no K^+ added (-K, this medium contained initially traces of K^+) or with 1000 µM K^+ added (+K); (**B**) and cross section of a stained root, ep: epidermis, c: cortex, e: endodermis, s: stele; (**C**) Leaves of 14 days-old seedlings **;** (**D**) Flower and anthers of mature plants grown in sufficient K^+-conditions.

Figure 3: K^+ content in 30 days-old plants supplied during 12 days with a nutrient solution containing 10, 100 or 3000 µM K^+. Data for (**A**) Shoot and (**B**) Roots are means ± SD (*n* =11-12). ANOVA analyses were performed to compare K^+ content between lines for each level of K^+ supply (NS, Non-Significant; ** and *** Significant at the α = 0.01 and 0.001 level respectively). Different letters indicate significant differences between means (Tuckey post-hoc test, *P*-value < 0.05).

Figure 4: Sensitivity to Cs^+ in *kup9* mutant lines. (**A**) 10 days-old seedlings grown in 8 mL of low K^+ (10 µM) or sufficient K^+ (1000 µM) nutritive solution and containing Cs^+. (**B**) Primary root elongation of 11 days-old seedlings grown in agar plates in the presence of Cs^+ and 14-40 µM K^+ or 1000 µM K^+. Plants were allowed to grow on MS½ agar plates during 4 days before transfer on Cs^+. Data are means ± SD (*n* =10-16).

Figure 5: Accumulation of Cs^+ in *kup9* mutant lines. (**A**) Cs^+ accumulation in 30 days-old plants exposed during 7 days to a nutrient solution containing 1 µM Cs^+ and 10 µM K^+ or 3000 µM K^+. Data are means ± SD (*n* = 6-8). (**B**) Cs^+ exchanges between 30 days-old plants and the external solution. External Cs^+ concentrations were followed by taking up small samples of the solution. Data are means ± SD (*n* = 5). (**B1**) Cs^+ depletion due to uptake by plants in a K^+-free solution (statistics are shown in **Table S2**). Before the experiment, plants were grown with low K^+-supply (10 µM) during 7 days to improve Cs^+ influx. (**B2**) Cs^+ released from contaminated plants to a Cs^+-free solution.

Figure 6: Model for Cs^+ transport in roots of *A. thaliana* depending on the level of K^+ supply. INFLUX. As for other cations, Cs^+ taken up by plants from the soil solution is transported across the root mainly through the symplastic pathway. Non-selective Cation Channels (NSCC, White and Broadley 2000, Hampton et al. 2005) and the high-affinity K^+ transporter HAK5 (Qi et al. 2008) are thought to mediate the major part of Cs^+ influx in sufficient (mM range) and low (µM range) K^+ conditions respectively. ABCG37 and ABCG33 mediate a significant part of Cs+ influx regardless the K^+ level (Ashraf et al., 2021). TRANSLOCATION. Cs^+ is highly mobile within plants. From the roots, Cs^+ is loaded into the xylem and distributed towards the aerial parts through yet unidentified transport systems. The Major Facilitator Superfamily transporter ZIFL2 has been proposed to prevent Cs^+ xylem loading mediating Cs^+ release into the apoplasm of endodermis and pericycle, under Cs^+ and K^+ excess (Remy et al. 2015). COMPARTMENTATION. Regarding its intracellular distribution, analyses of contaminated plant cells revealed that Cs^+ is not limited to the cytosol but is also found in vacuole and probably chloroplasts (Le Lay et al. 2006, Akamatsu et al. 2014). Identities of transport systems involved in these mechanisms are unknown. EFFLUX. Given our results, we propose three hypotheses

involving KUP9 in the limitation of Cs^+ accumulation (see in text) either speculating that KUP9 could work as an efflux carrier (HYP. A and B) or that KUP9 could affect transport of Cs+ through others carriers (HYP. C).
Cyt: cytosol, Org: Organelles.

Figure 7: Phylogenetic organization of the KUP/HAK/KT transporters family in *Arabidopsis thaliana*. The phylogenetic tree was generated from polypeptide sequences with the PhyML software (v3.0) in the online platform Phylogeny.fr (« One Click » mode with Muscle for alignment and Gblock for alignment curation, http://www.phylogeny.fr/simple_phylogeny.cgi). The unrooted tree was drawn with the online software PONYTREE (website under construction). Bootstrap values (in percentage) are indicated at the corresponding nodes and the scale represents the number of changes per 100 amino acid. Polypeptide sequences of AtKUP9 homologs (Al7g33950, Sp7g18400 and Sp7g12130) and AtKUP/HAK/KT were from thellungiella.org (http://thellungiella.org), Phytozome (https://phytozome.jgi.doe.gov/pz/portal.html) and TAIR database (https://www.arabidopsis.org/).

Table 1: Rb^+ accumulation in 30 days-old *Arabidopsis thaliana* plants exposed during 7 h to 20 mL of a K^+-free nutrient solution containing 50 µM RbCl. Before experiment, plants were supplied with a 10 µM K^+ nutrient solution during 5 days to enhance subsequent Rb^+ uptake. Data are means ± SD (n=5). Different letters indicate significant differences between means.

Lines	Shoot Rb^+ content (µmol g^{-1} DW)	Roots Rb^+ content (µmol g^{-1} DW)
Col-0	0.55 ± 0.20 **(a)**	5.13 ± 0.95 **(b)**
kup9-1	0.75 ± 0.30 **(a)**	5.37 ± 1.37 **(b)**
kup9-3	0.73 ± 0.30 **(a)**	6.63 ± 0.95 **(b)**

Table 2: Cs^+ Root:Shoot concentration ratio in plants exposed during 7 days to a nutrient solution containing 1 µM CsCl and 10 µM K^+ or 3000 µM K^+. Data are means ± SD (n=6-8).

Lines	Cs^+ Root:Shoot concentration ratio	
	Low K^+ supply (10 µM)	Sufficient K^+ supply (3000 µM)
Col-0	16.7 ± 4.9	1.4 ± 0.1
kup9-3	19.9 ± 3.0	1.5 ± 0.4
kup9-1	15.9 ± 2.6	1.2 ± 0.2
hak5-3	3.8 ± 0.8	1.2 ± 0.2

Table 3: Relative expression of *HAK5* in wildtype Col-0 and in *kup9* plants supplied with distinct levels of K^+. Experiments were performed on 29-34 days-old plants grown in hydroponics with three distinct levels of K^+: 10 (low), 100 (intermediate) or 3000 µM (taken as reference) during 7 days. Expression levels of *HAK5* were calculated relative to the *ROC3* gene after RT-qPCR analysis of cDNA synthesized from roots total RNA. Fold change given here are related to *HAK5* expression in plants supplied with 3000 µM K^+, different letters indicate statistically significant differences (*t*-test). *P*-value: statistical significance of differential *HAK5* expression in plants supplied with 10 or 100 µM compared with plants grown in 3000 µM K^+. SD: associated with the fold change based on three replicate experiments.

K^+supply (µM)	Lines	*P*-value	Fold change	SD
10	Col-0	1.16×10^{-5}	11.9	1.3
	kup9-3	9.46×10^{-5}	13.3	3.1
	kup9-1	1.16×10^{-7}	14.3	3.8
100	Col-0	0.42	1.5 **(a)**	1
	kup9-3	0.01	4.1 **(b)**	1.1
	kup9-1	0.01	3.3 **(b)**	0.4

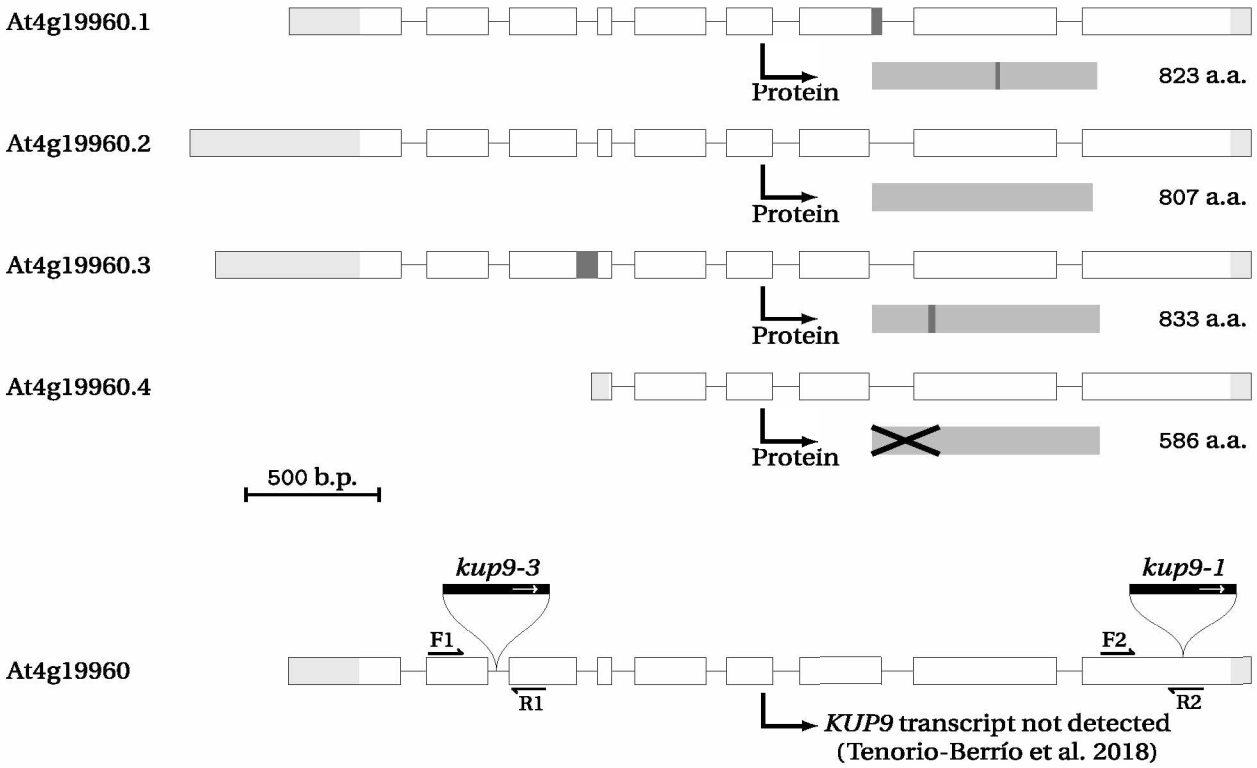

Figure 1: *KUP9* gene model and T-DNA insertion sites in *kup9-1* (SALK_108080C) and *kup9-3* (SAIL_211_E04) mutant lines. White boxes represent exons whereas dark lines between boxes denote introns of *AtKUP9* gene; light grey boxes represent 3' and 5'-UTR. The current *KUP9* gene model implies four distinct splice variants (The Arabidopsis Information Resource, TAIR, www.arabidopsis.org/servlets/TairObject?id=127288&type=locus, on www.arabidopsis.org, May 07, 2020). Dark grey boxes highlight changes between the different splicing variants (for the AT4g19960.4 model, the absence of amino acids at the beginning of the predicted protein is marked with a cross). For *kup9* mutant lines, T-DNA insertions are outlined by large triangle and black arrows represent gene specific primers used for mutant lines checking (F1: GGAGATTTAGGGACGTCTCCATTGTATGTG, R1: TCCTCATCACTACGGTGCTGATTCG; F2: CCTACAGCAGCACGTATTCCGTCAAC, R2: CGGTGTTCCCCATTATATGAACAACACCTG).

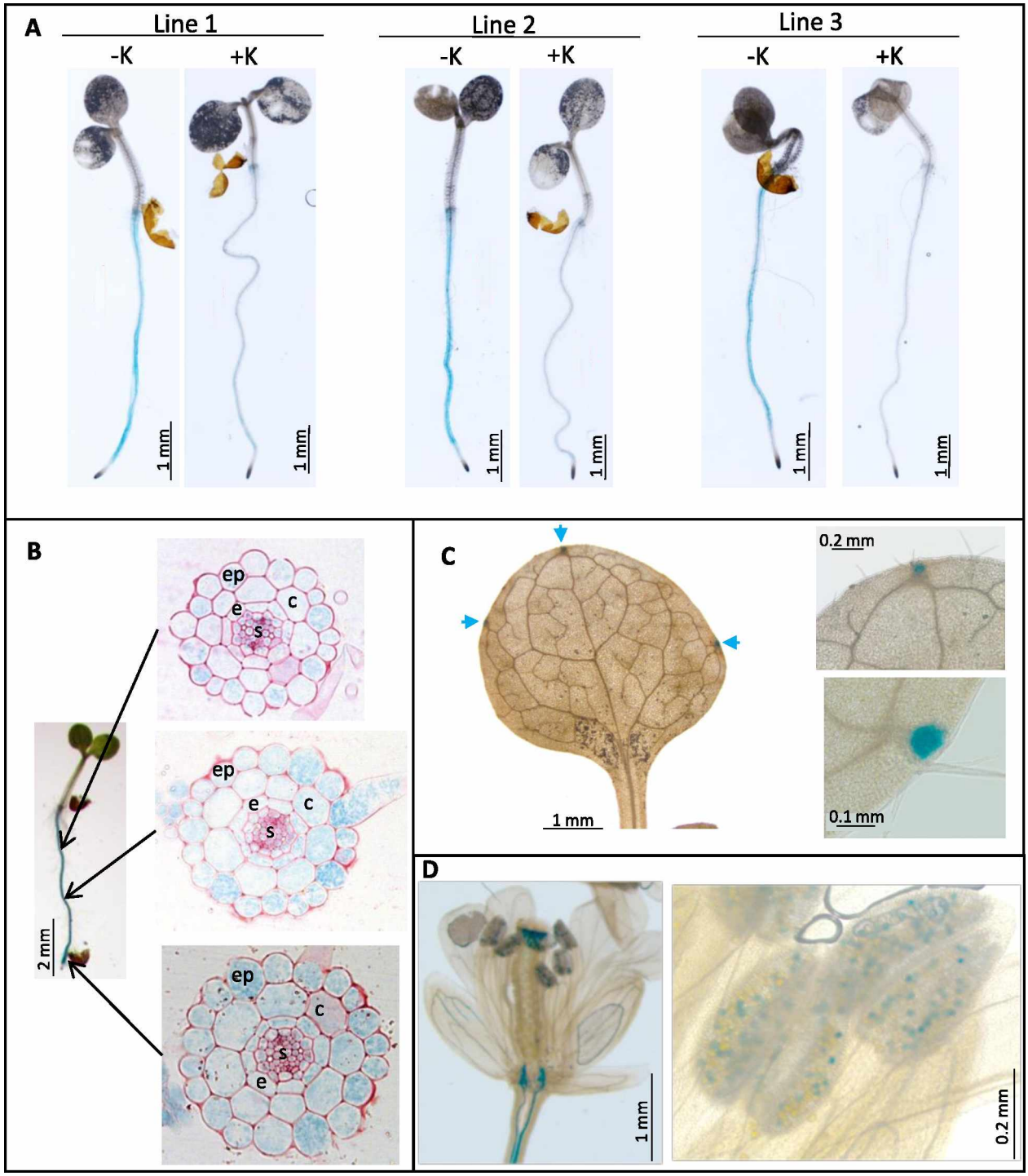

Figure 2: Spatial transcription pattern of *KUP9* determined in *ProKUP9:GFP-GUS* transgenic *A. thaliana* plants. GUS staining of (**A**) Roots of 7 days-old seedlings grown in nutritive agar medium with no K^+ added (-K, this medium contained initially traces of K^+) or with 1000 µM K^+ added (+K); (**B**) and cross section of a stained root, ep: epidermis, c: cortex, e: endodermis, s: stele; (**C**) Leaves of 14 days-old seedlings **;** (**D**) Flower and anthers of mature plants grown in sufficient K^+-conditions.

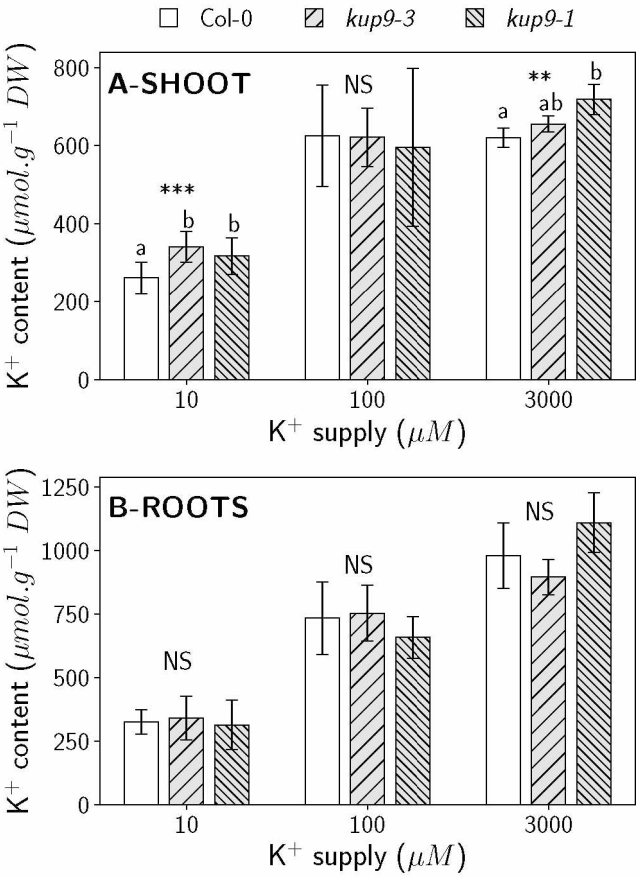

Figure 3: K^+ content in 30 days-old plants supplied during 12 days with a nutrient solution containing 10, 100 or 3000 µM K^+. Data for (**A**) Shoot and (**B**) Roots are means ± SD (n=11-12). ANOVA analyses were performed to compare K^+ content between lines for each level of K^+ supply (NS, Non-Significant; ** and *** Significant at the α = 0.01 and 0.001 level respectively). Different letters indicate significant differences between means (Tuckey post-hoc test, *p*-value < 0.05).

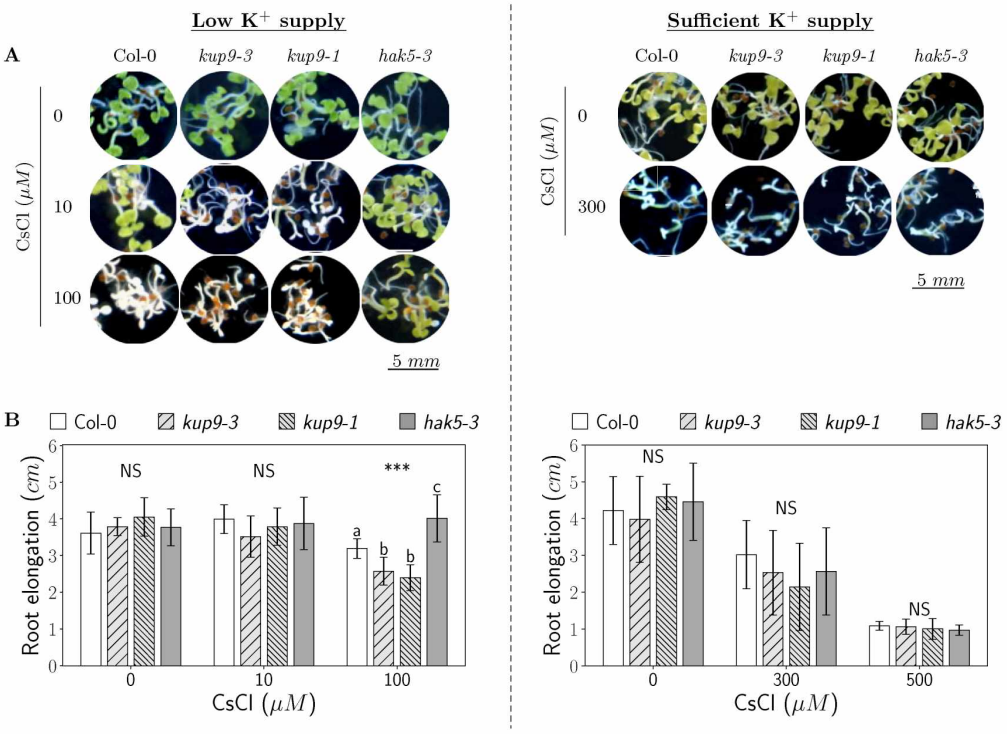

Figure 4: Sensitivity to Cs^+ in *kup9* mutant lines. (**A**) 10 days-old seedlings grown in 8 mL of low K^+ (10 µM) or sufficient K^+ (1000 µM) nutritive solution and containing Cs^+. (**B**) Primary root elongation of 11 days-old seedlings grown in agar plates in the presence of Cs^+ and 14-40 µM K^+ or 1000 µM K^+. Plants were allowed to grow on MS½ agar plates during 4 days before transfer on Cs^+. Data are means ± SD (n=10-16).

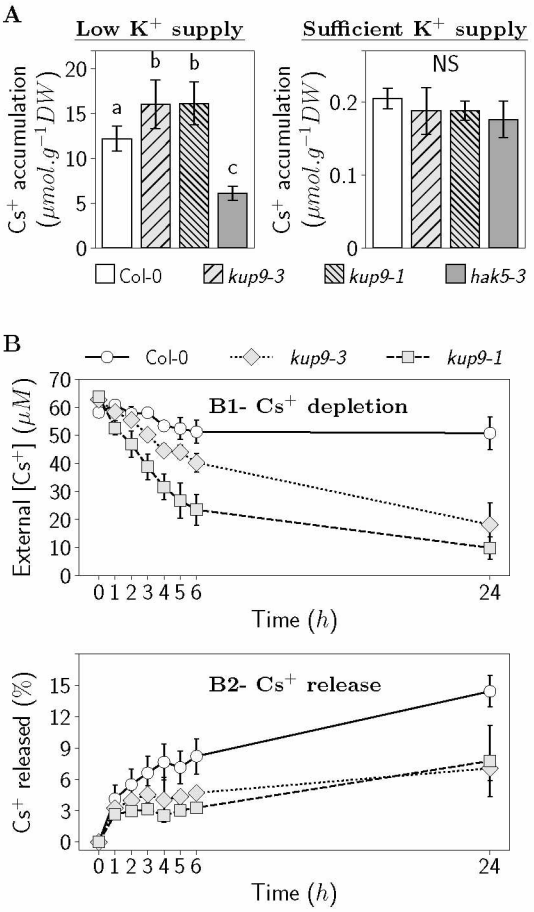

Figure 5: Accumulation of Cs^+ in *kup9* mutant lines. (**A**) Cs^+ accumulation in 30 days-old plants exposed during 7 days to a nutrient solution containing 1 µM Cs^+ and 10 µM K^+ or 3000 µM K^+. Data are means ± SD (n=6-8). (**B**) Cs^+ exchanges between 30 days-old plants and the external solution. External Cs^+ concentrations were followed by taking up small samples of the solution. Data are means ± SD (n=5). (**B1**) Cs^+ depletion due to uptake by plants in a K^+-free solution. Before the experiment, plants were grown with low K^+-supply (10 µM) during 7 days to improve Cs^+ influx. (**B2**) Cs^+ released from contaminated plants to a Cs^+-free solution.

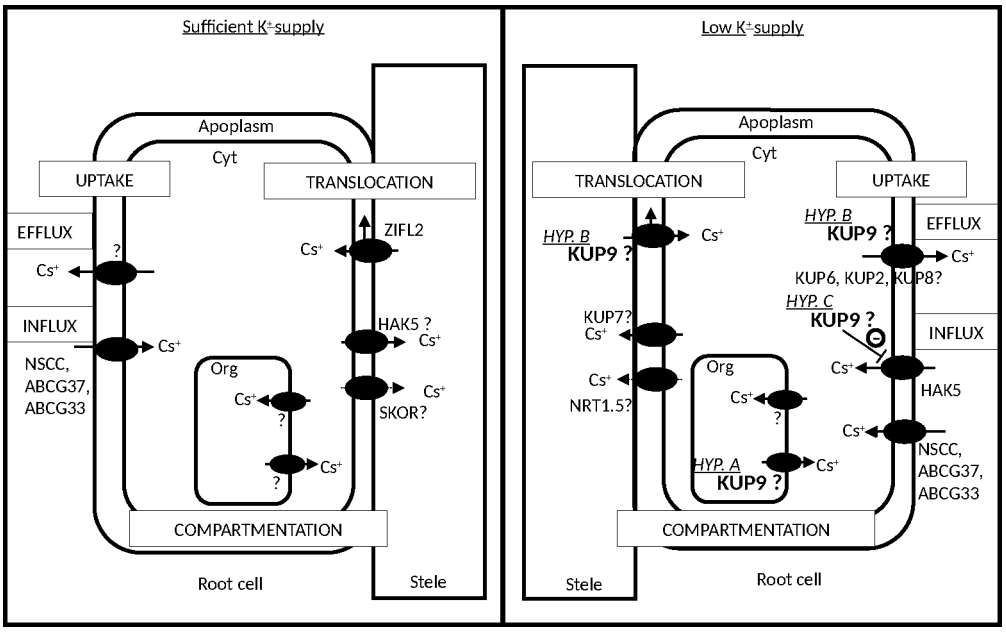

Figure 6: Model for Cs^+ transport in roots of *A. thaliana* depending on the level of K^+ supply. INFLUX. As for other cations, Cs^+ taken up by plants from the soil solution is transported across the root mainly through the symplastic pathway. Non-selective Cation Channels (NSCC, White and Broadley 2000, Hampton et al. 2005) and the high-affinity K^+ transporter HAK5 (Qi et al. 2008) are thought to mediate the major part of Cs^+ influx in sufficient (mM range) and low (µM range) K^+ conditions respectively. ABCG37 and ABCG33 mediate a significant part of Cs+ influx regardless the K^+ level (Ashraf et al., 2021). TRANSLOCATION. Cs^+ is highly mobile within plants. From the roots, Cs^+ is loaded into the xylem and distributed towards the aerial parts through yet unidentified transport systems. The Major Facilitator Superfamily transporter ZIFL2 has been proposed to prevent Cs^+ xylem loading mediating Cs^+ release into the apoplasm of endodermis and pericycle, under Cs^+ and K^+ excess (Remy et al. 2015). COMPARTMENTATION. Regarding its intracellular distribution, analyses of contaminated plant cells revealed that Cs^+ is not limited to the cytosol but is also found in vacuole and probably chloroplasts (Le Lay et al. 2006, Akamatsu et al. 2014). Identities of transport systems involved in these mechanisms are unknown. EFFLUX. Given our results, we propose three hypotheses involving KUP9 in the limitation of Cs^+ accumulation (see in text) either speculating that KUP9 could work as an efflux carrier (HYP. A and B) or that KUP9 could affect transport of Cs+ through others carriers (HYP. C).

Cyt: cytosol, Org: Organelles.

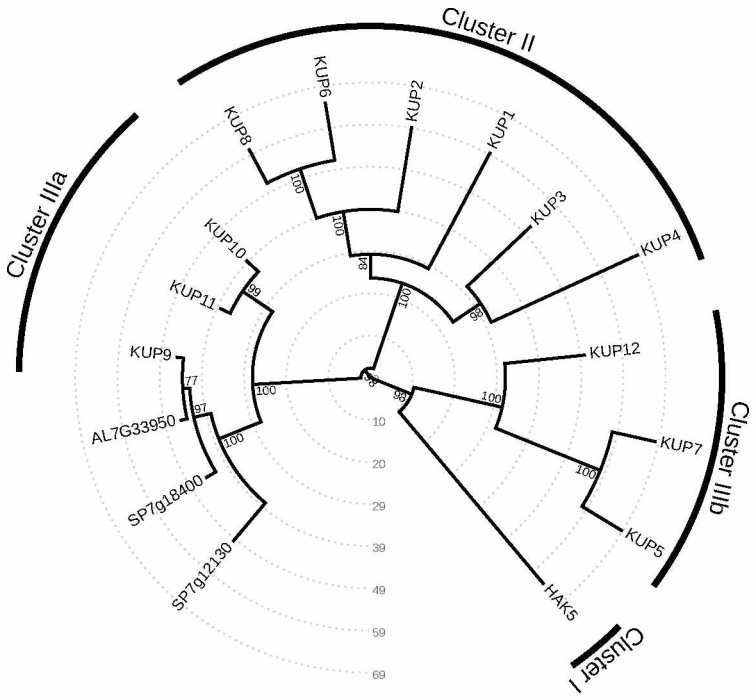

Figure 7: Phylogenetic organization of the KUP/HAK/KT transporters family in *Arabidopsis thaliana*. The phylogenetic tree was generated from polypeptide sequences with the PhyML software (v3.0) in the online platform Phylogeny.fr (« One Click » mode with Muscle for alignment and Gblock for alignment curation, http://www.phylogeny.fr/simple_phylogeny.cgi). The unrooted tree was drawn with the online software PONYTREE (website under construction). Bootstrap values (in percentage) are indicated at the corresponding nodes and the scale represents the number of changes per 100 amino acid. Polypeptide sequences of AtKUP9 homologs (Al7g33950, Sp7g18400 and Sp7g12130) and AtKUP/HAK/KT were from thellungiella.org (http://thellungiella.org), Phytozome (https://phytozome.jgi.doe.gov/pz/portal.html) and TAIR database (https://www.arabidopsis.org/).

SUPPORTING INFORMATION

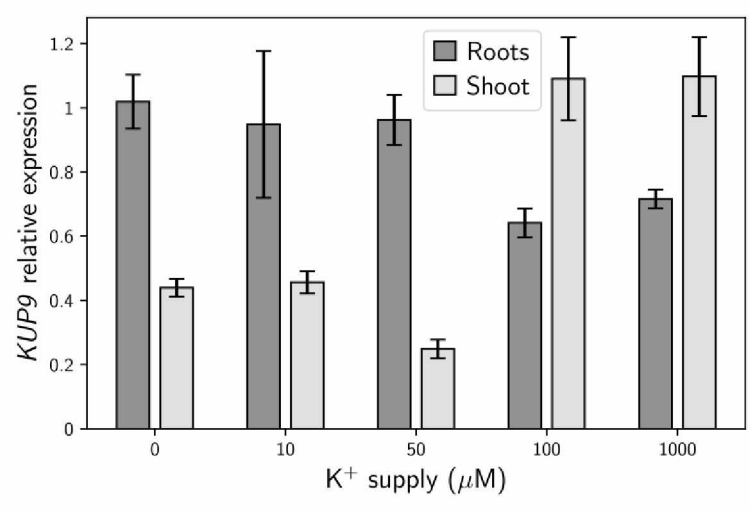

Figure S1: *KUP9* relative expression measured in RT-qPCR. Total RNA of roots and shoots from Col-0 supplied with different amount of K^+ (0, 10, 50, 100 or 1000 µM) was extracted using the RNeasy™ kit (QIAgen) according to the manufacturer's instructions. Reverse transcription of mRNA was performed over 1 µg of total RNA using SuperScript™ Vilo™ kit (Invitrogen) with oligo(dT)$_{20}$ primers. The synthesized cDNAs were analysed by quantitative real-time PCR using SYBR® Green I Master mix on a LightCycler® 480 (Roche). PCR amplifications of a *KUP9* fragment (forward primer: AGAGGAGGAGGAGACGGATGAG, reverse primer: GCCCTACAAATCTTAGCAAG) were performed at 95°C for 10 sec (45 cycles) and 60°C for 10 sec. Relative quantitative results were calculated after normalization to *ROC3*. Data are mean ± SD of a pool of three plants analysed three times.

Appendix S2- Localisation of KUP9 transporter

Correct expression of the GFP-KUP9 fusion protein in transgenic lines was checked by western blotting with an anti-GFP antibody. Total proteins were extracted from frozen roots, leaves and flowers pools of three transgenic plants in the fourth generation using an extraction buffer (50 mM Tris-Hcl pH 8.5, 5 mM EDTA NaOH pH 8.2, 2 mMdithiotreitol, 1X protease inhibitor cocktail). After centrifugation, membrane protein fraction was treated separately in a resuspension buffer (25 mM Tris-HCL pH 8, 2 mM DTT, 0.5% Triton X-100, 1X protease inhibitor cocktail) by sonication (4 cycles of 10 sec ON and 10 sec OFF, 10% of the maximal amplitude, keeping on ice).

Denaturing electrophoresis (Invitrogen™Novex™ Mini Cell, 80V, 2 h, running buffer: 25 mM Tris-HCl pH 8, 192 mM glycine, 0.1% SDS) was performed on 45 µg of proteins mixed with NuPage® reactive and loaded in polyacrylamide gel (stacking/ separating part: 5%/ 8% acrylamide, 125 mM / 375 mM Tris pH 6.8 / 8.8, 0.1% SDS, 0.1% ammonium persulfate, 0.1% / 0.08% TEMED).

Polyacrylamide gel carrying proteins was placed in contact with a nitrocellulose membrane and sandwiched between two layers of Scotch-Brite™ and Whatman® filter paper. Denatured and charged proteins were transferred from gel to nitrocellulose membrane by electroblotting(32 V) performed overnight at 4°C in a tank filled with a transfer buffer (25 mM Tris-HCl pH 8, 192 mM glycine, 0.1 % SDS, 20% ethanol).

Nitrocellulose membrane carrying the transferred proteins was saturated during 1 h with a TBS-T solution (50 mM Tris, 150 mMNaCl, 5% milk powder, pH 7.6, 0.1% Tween), incubated during 2 h in TBS-T with an anti-GFP antibody (200 $ng.\mu L^{-1}$ of a monoclonal antibody produced in mouse, Living Colors® A.v. JL-8, Clontech), rinsed in TBS-T and incubated during 20 min in TBS-T with secondary antibody (140 $ng.\mu L^{-1}$ of a rabbit anti-mouse antibody-HorseRadish Peroxidase). Finally, chimiluminescence analysis was performed in a G:box after membrane incubation following manufacturer's instructions (SuperSignal™ West Pico kit).

Despite several observations on various samples, we were not able to detect the GFP signal in transgenic plants carrying the pro*35S*:*GFP-KUP9* and pro*KUP9*:*GFP-KUP9*.Transient expressionassays on *A. thaliana* mesophyll protoplast did not provide further results.The correct transcription of the transgene was confirmed by PCR (**Fig. S2**) and sequencing of the amplified fragment (data not shown). Nevertheless, immunedetection performed in transgenic lines carrying the two constructs with an anti-GFP antibody (**Fig. S2**) revealed that the 120 kD expected GFP-KUP9 fusion protein was cleaved.

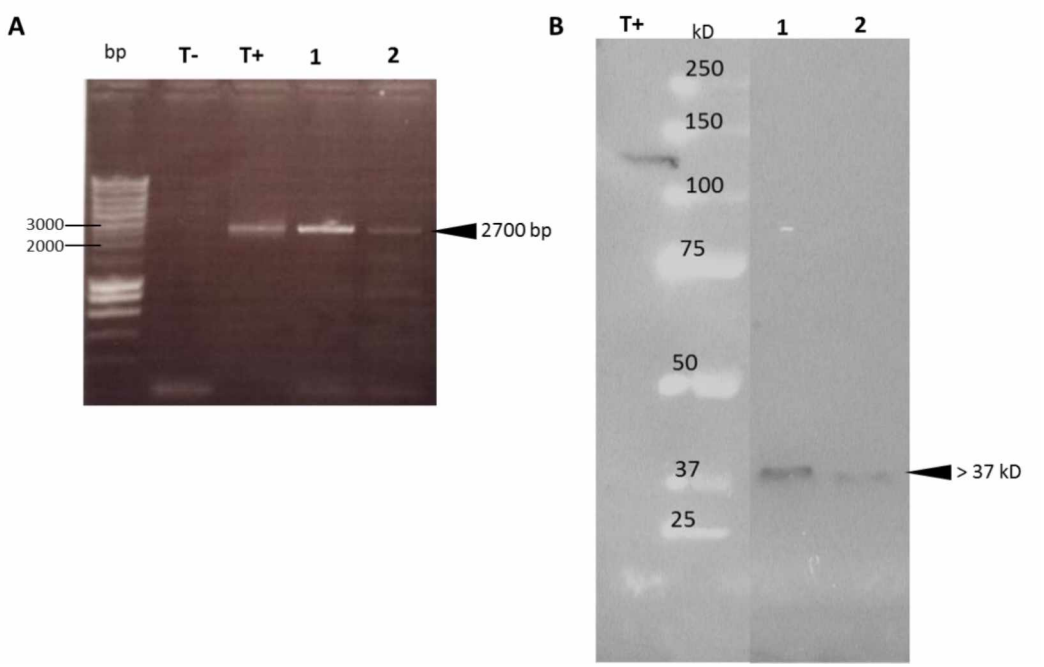

Figure S2: Check of pro*35S*:*GFP-KUP9* and pro*KUP9*:*GFP-KUP9* constructs in transgenic lines. **(A)** Correct transcription of the transgene was confirmed using PCR on cDNA from transgenic lines combining a *GFP* specific primer (AAGCAGAAGAACGGCATCAAGG) and a CDS *KUP9* specific primer (GCTGCTGTAGGTGCTTGAGTTTG). T-: Col-0 cDNA, T+: Miniprep of *E. coli* containing pro*35S*:*GFP-KUP9* construct, 1: cDNA from a transgenic lines carrying the pro*35S*:*GFP-KUP9* construct, 2: cDNA from a transgenic lines carrying the pro*KUP9*:*GFP-KUP9* construct. **(B)** Immunodetection of the GFP-KUP9 fusion protein using anti-GFP antibodies on total proteins extracted from transgenic lines. T^{+}: control proteins extracted from a transgenic yeast strain expressing a protein fused with GFP reporter, 1: proteins extracted from transgenic plants carrying the pro*35S*:*GFP-KUP9* construct, 2: proteins extracted from transgenic plants carrying the pro*KUP9*:*GFP-KUP9* construct.

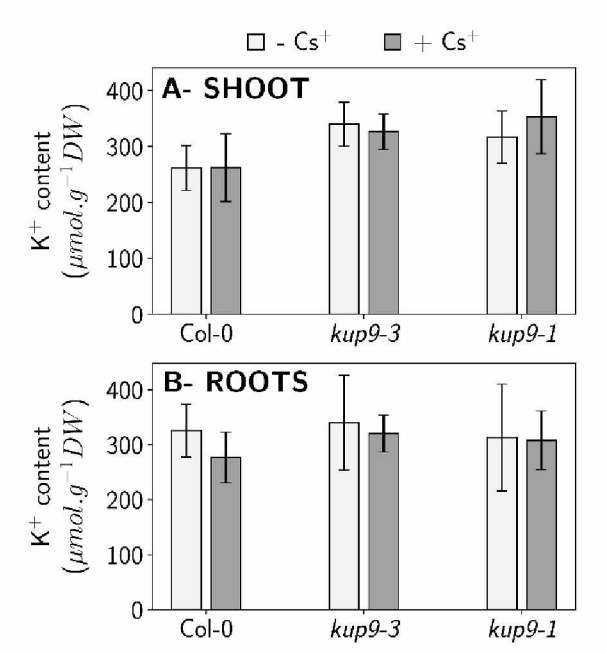

Figure S3: K^+ content in Cs^+-exposed plants. K^+ content was measured in 30 days-old plants supplied during 12 days with a nutrient solution containing 10 µM K^+ and exposed during 7 days to 1 µM Cs^+ (+ Cs_+) or not exposed (- Cs_+). Data for (A) Shoot and (B) Roots are means ± SD (n=11-12). ANOVA analyses performed to compare K^+ content between lines for each level of K^+ supply revealed no significant differences.

Table S1: Cs^+ concentrations (µmol.g^{-1} dry weight) in shoots and roots of 30 days-old *Arabidopsis thaliana* plants exposed during 7 days to a nutrient solution containing 1 µM Cs^+ and 10 µM or 3000 µM K^+. Data are means ± SD (n=6-8).

Lines	Low K^+ supply (10 µM)		Sufficient K^+ supply (3000 µM)	
	Cs^+ in shoots	Cs^+ in roots	Cs^+ in shoots	Cs^+ in roots
Col-0	1.96 ± 0.86	29.48 ± 7.46	0.19 ± 0.01	0.27 ± 0.02
kup9-3	2.41 ± 0.63	46.52 ± 7.26	0.17 ± 0.03	0.24 ± 0.04
kup9-1	2.81 ± 0.37	44.32 ± 7.15	0.18 ± 0.02	0.21 ± 0.03
hak5-3	3.92 ± 0.45	14.87 ± 3.51	0.16 ± 0.03	0.19 ± 0.03

Table S2: Adjusted p-values from Tukey HSD post-test for Cs^+ depletion assays presented in Figure 5.B1.

Lines	1 h	2 h	3 h	4 h	6 h	24 h
Col-0 vs *kup9-1*	0.2299	0.4329	0.0121	0.0098	0.0758	0.0196
Col-0 vs *kup9-2*	0.0005	0.0003	0.00001	0.000009	0.00005	0.00002
kup9-1 vs *kup9-2*	0.0085	0.0025	0.0015	0.0010	0.0017	0.0019